PHYSICAL REVIEW B VOLUME 13, NUMBER 3 1 FEBRUARY 1976

Lattice-site location of ion-implanted impurities in copper and other fcc metals

J. A. Borders*
Sandia Laboratories, Albuquerque, New Mexico 87115

J. M. Poate
Bell Laboratories, Murray Hill, New Jersey 07974
(Received 25 August 1975)

The backscattering-channeling technique has been used to study the lattice location of various heavy atoms implanted in a channeling direction to high doses in copper and other fcc metals. Gold implanted into Cu, Pd, and Ag is found to be $(100 \pm 1)\%$ on substitutional sites (in Ni, Au is 96% substitutional). Investigations of the lattice location of heavy metallic atoms implanted in Cu (Ag, Sb, W, Pt, Au, Hg, Tl, Pb, and Bi) show that these impurities occupy with a high probability ($\geq 60\%$) regular fcc lattice sites for atomic concentrations $\lesssim 1\%$. In contrast, I shows a lower probability for occupying Cu lattice sites and the substitutionality is a function of depth, whereas Xe is entirely nonsubstitutional. There is no implantation temperature dependence of the substitutionality of Au, W, or Xe in Cu between 15 K and room temperature. These results are compared with criteria such as the size, electronegativity, and the binary phase diagrams of the implanted systems involved, but it is concluded that the final position of metallic atoms is determined mainly by nonequilibrium processes occurring near the end of the ion range. For atomic concentrations $> 10\%$, Au remains 100% substitutional in Cu but W produces a highly disordered layer in which the W atoms occupy no regular lattice site. Low levels of damage are seen in the host copper crystals after high-dose channeled implantations of heavy ions. The results indicate an absence of displaced host atoms and a layer of dechanneling centers which is approximately coincident in depth with the implanted species. These results suggest that lattice strain around the implanted atoms is the major cause of dechanneling.

I. INTRODUCTION

Classical metallurgy deals with systems produced at equilibrium, or at least at quasiequilibrium. Recent applications of ion-implantation techniques, developed for the controlled shallow doping of semiconductors, to metals have brought us to the realm of nonequilibrium metallurgy processes. Energetic ions can be implanted in a metal surface layer without regard for solubility limits, but subject only to sputtering considerations. Under these nonequilibrium conditions, the physical states of the implanted atoms within the target are of interest. Also of interest is the effect of the damage created in the host material as the impinging ions are slowed to rest. Both the chemical alloying effects of the implanted impurities and the damage may produce surface layers in the host which have very different physical properties from the host itself. This is one of the reasons for the current effort in investigating the effects of ion beams on metals.[1]

One of the most important properties of an impurity atom is its location within a host crystal. Ion channeling is a mechanism by which an incident ion beam can selectively sample various crystallographic locations within a host crystal and in many cases make direct measurements of impurity-atom lattice locations. The channeling technique for lattice location has been discussed in detail elsewhere.[2,3] This technique is particularly applicable to determining the lattice location of heavy impurities introduced by ion implantation into lighter host materials.

A number of implanted-metal crystal systems have been investigated by channeling[4]; however, until recently[5,6] no implanted impurity had been found which was 100% substitutional. In this paper we report the results of channeling investigations of the lattice location of a wide variety of implanted impurity atoms in copper and some related results on the damage introduced in the copper crystals by the implantations.

II. EXPERIMENTAL

Single-crystal slices of high-purity copper were cut with a $\langle 110 \rangle$ axis approximately normal to the surface. The samples were lapped on 600 grit paper, followed by lapping on 23- and 8-μm SiC Ultralap abrasive sheets. To remove mechanical damage caused by cutting and lapping, each sample was polished on Politex pads saturated with Syton polishing solution. The resultant polished surfaces had a mirrorlike appearance and were relatively damage free. The Ni, Pd, and Ag crystals were prepared in a similar fashion. Random and $\langle 110 \rangle$ aligned spectra of each sample indicated minimum yields of 3%–5% for 1.8-MeV He^+. Most of the copper samples were electropolished following the Syton polishing. This was accomplished in a stirred 2:1 mixture of phosphoric acid and distilled water at room temperature. Typical cell voltages and polishing times were 1.75 V for 30 min. The electropolished copper samples con-

sistently had minimum yields of 2%–3%.

Implantations were carried out on one of four low-energy accelerators. At Murray Hill, Au, Pt, Hg, and Tl implants were performed using a 300-keV Ortec accelerator with a Hill-Nelson ion source. At Sandia, Au, Ag, Pb, Bi, Pt, and I implants were performed in a 300-keV Accelerators, Inc. machine with a Dan Physik 911 source, whereas the W, Xe, Cu, and Sb implants were done with an 80-keV Lintott accelerator or a 400-keV Van de Graaff accelerator using their standard ion sources. Unless otherwise specified, all crystals were aligned using 1.8-MeV He^+ channeling prior to implantation and the implants carried out in a ⟨110⟩ channeling direction.

The crystal alignment for low-energy heavy-ion implantation is not critical and in good crystals it is difficult to avoid channeled implants. Initial experiments with intentional misalignment of 7° between the implantation beam and the ⟨110⟩ axis showed very deep impurity penetration and damage depths compared to Lindhard-Scharff-Schiøtt (LSS) ranges. Implants could be performed in which the range corresponded to LSS theory, but the choice of implant direction was critical. Cairns *et al.*[7] have used characteristic x-ray generation to measure critical angles for 150–350-keV rare-gas ion channeling in ⟨110⟩ copper. They find their data can be fitted to a critical-angle formula due to van Wijngaarden[8] which uses an inverse-square-law fit to a screened Coulomb potential

$$\psi_{IS} = \left(\frac{a}{2.71d}\ \psi_1^2\right)^{1/3} ,$$

where a is the Thomas-Fermi screening distance, d is the atom spacing along the crystal row, and ψ_1 is the Lindhard[9] high-energy critical angle given by

$$\psi_1 = (2Z_1Z_2e^2/dE)^{1/2} .$$

For one of the systems described in this paper, 150-keV Au in ⟨110⟩ Cu, a/d is about 0.035, ψ_1 is about 24°, and ψ_{IS} is 7.5°. Thus the channeling critical angles have a full width of about 15° if this model is accurate. For uniformity, experimental ease, and to avoid ambiguities caused by not knowing how much of the beam was channeled, all implants were done within ±0.5° of the ⟨110⟩.

The analysis beams of $^4He^+$ ions were produced by 2-MeV Van de Graaff accelerators at Albuquerque and Murray Hill. The incident helium beams were collimated to achieve angular divergence half-angles of better than 0.05°. The scattered ions were detected and analyzed with silicon surface-barrier detectors and associated nuclear electronics with a total system resolution for 1–2-MeV He^+ ions of 12–15 keV. Both electronics systems were equipped with pulse-pile-up-rejection circuitry.[10]

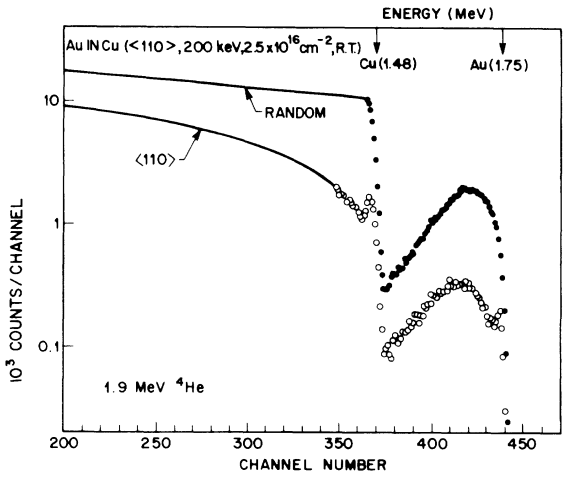

FIG. 1. Random and ⟨110⟩-aligned spectra of Cu implanted at room temperature with 1.0×10^{16} cm^{-2} 200-keV Au atoms. The implant was performed in the ⟨110⟩ channeling direction. 2.5×10^{16} Au cm^{-2} were actually retained in the sample.

Two separate goniometers were equipped for *in situ* low-temperature implantation and analysis. One system used a liquid-helium transfer refrigerator to achieve sample temperatures below 10 K. The second system used a helium-gas mechanical refrigerator to cool the goniometer-mounted sample to 40–60 K. In both cases the samples were surrounded by shields cooled by liquid nitrogen and chamber vacuums were $1–4\times10^{-7}$ Torr.

III. RESULTS

A. Au in Cu and other fcc metals

Figure 1 shows the random and ⟨110⟩-aligned spectra for a 200-keV Au ⟨110⟩ channeled room-temperature implantation at a dose of 10^{16} cm^{-2} into Cu. The large reduction of the Cu and Au scattering yields when the ^4He beam is aligned with the ⟨110⟩ crystal axis indicates that: (i) the Cu crystal has suffered little lattice damage by the Au implantation, and that (ii), the Au atoms are highly substitutional. These spectra are typical of those obtained from all the metal implants into single-crystal fcc metals described here with minor differences in damage levels and implanted impurity depth distributions. The implanted Au can be seen from Fig. 1 to extend deeply into the Cu crystal. The depth of the maximum in the Au distribution, corresponding to 3 at.%, is ~800 Å; however, the concentration of Au is still 0.3 at.% at a depth of ~2500 Å where the scattering from Au atoms cannot be distinguished from scattering from surface copper. If we extrapolate the gold distribution to zero concentration, the implanted

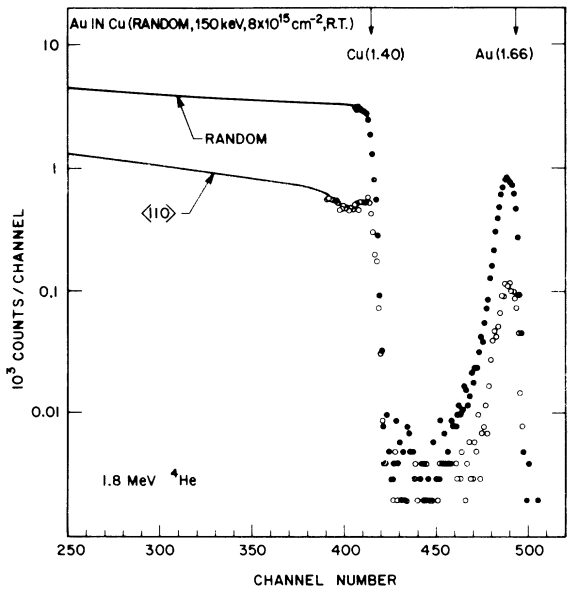

FIG. 2. Random and ⟨110⟩-aligned spectra of Cu implanted at room temperature with 1.0×10^{16} cm^{-2}, 150-keV Au atoms. The implant was performed 17° off the ⟨110⟩, $\frac{3}{14}$ of the way from the {113} to the {100}. 8×10^{15} Au cm^{-2} were actually retained in the sample.

gold extends ~4500 Å into the Cu. The LSS projected range[11] for 200-keV Au in Cu is 214 Å with a rms spread of 74 Å, and thus the observed distributions extend far beyond the LSS range. That this effect is due to channeling of the Au in the Cu is confirmed by the data of Fig. 2 which shows the random and ⟨110⟩-aligned spectra for 150-keV Au implanted 17° from the ⟨110⟩ axial channel along a plane $\frac{3}{14}$ of the way from the {113} to the {100}. The distribution in this case shows a maximum at a range of ~200 Å approximately the LSS projected range of 170 Å,[11] indicating that the extended distributions observed in the data of Fig. 1 can be attributed to channeling. As discussed previously, because of the difficulty in finding a truly random direction, crystals used for the rest of this study were aligned prior to implantation using 1.8-MeV He^+ and implanted in a ⟨110⟩ channeling direction.

For lattice-location measurements using ion channeling, the substitutionality of an implanted species can be defined as

$$S=\frac{1-\chi_{min}(\text{impurity})}{1-\chi_{min}(\text{host})}\ ,$$

where χ_{min} is the ratio of the aligned to random scattering yields for the respective species. Using the above equation and the data shown in Fig. 1, the substitutionality of implanted Au in Cu is 100%±3%. This was the first reported case of 100% substitutionality for room-temperature implanted species with no annealing.[5] In the case of the random implant (Fig. 2), the substitutionality is also 100% and thus, at least for the case of Au in Cu, the results are independent of the direction of the implant. It should be noted that for the fcc lattice, measurements of the ⟨100⟩ and ⟨111⟩ directions are unnecessary if the ⟨110⟩ channeling results indicate 100% substitutionality.

More accurate estimates of the lattice site location can be obtained by comparing the normalized angular dependence of the scattering yield at a given depth for both host and impurity.[10] The initial parts of this study[5,6] indicated that Au implanted into four fcc metals (Ni, Cu, Pd, and Ag) was 100%±1% substitutional. Figure 3 shows angular distributions for these four cases where the angles have been plotted in units of $\psi_{1/2}$. The angular distributions of Au in Cu, Pd, and Ag are seen to exactly duplicate the distributions of the respective hosts to within experimental error indicating complete substitutionality. Au in Ni is seen to be 96% substitutional. It should be noted, however, that the host χ_{min} have increased substantially over the unimplanted values. We will suggest later that this increase in χ_{min} is due to

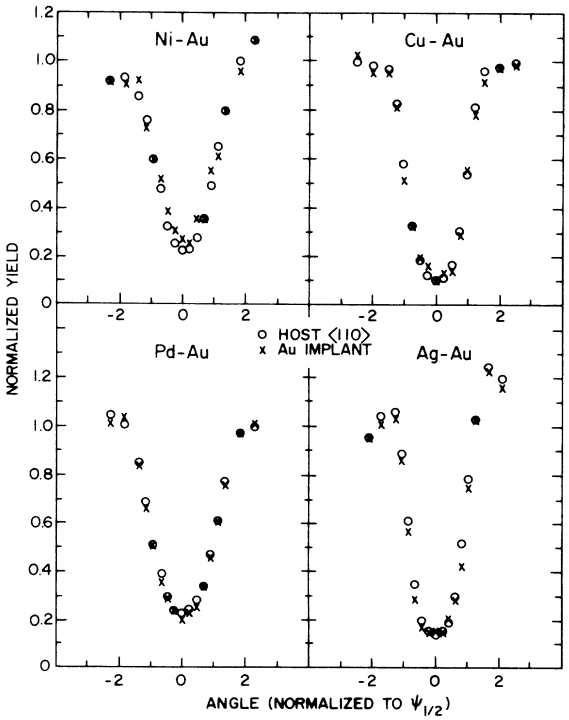

FIG. 3. Channeling angular distributions of Ni, Cu, Pd, and Ag crystals implanted at room temperature with ~10^{16} cm^{-2}, 200-keV Au atoms. The open circles are the host scattering and the ×'s correspond to the Au scattering.

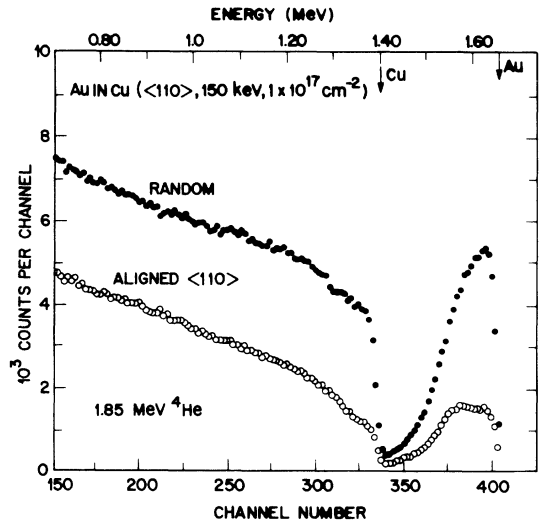

FIG. 4. Random and ⟨110⟩-aligned spectra of Cu implanted along the Cu ⟨110⟩ at room temperature with 1×10^{17} cm^{-2}, 150 keV Au atoms.

lattice strain associated with the implanted impurities.

The data listed above are for Au implants of 10^{16} Au cm^{-2}. The peak concentrations of Au created by these implants are 2–3 at.%. To examine whether complete substitutionality could be achieved for implants which create higher concentrations of the implanted species, 150-keV Au was implanted into Cu to a nominal dose of 1×10^{17} cm^{-2}. The channeling spectra from this sample are shown in Fig. 4. The depth distribution of the Au is beginning to become somewhat narrower than the depth distribution for 10^{16} Au cm^{-2} shown in Fig. 1. This is probably due to the increased damage in the crystal and greater dechanneling of the Au ions. The peak concentration of Au from the data of Fig. 4 is ~17 at.% and the amount of Au actually retained in the sample is 1.4×10^{17} cm^{-2}. Owing to the channeled implant, practically all the implanted Au is probably retained. For this case also, the Au is found to be as substitutional as the copper lattice indicating that the Au is 100% (±1%) substitutional.

It should be pointed out that implant doses are discussed in two ways in this paper. Normally we use dose to refer to the implant dose calculated from the integrated charge incident on the sample, with suitable precautions for secondary electrons. In some cases, however, we refer to the amount of impurity retained in the target which is obtained by integrating the random scattering peak due to the impurity and comparing this with the host scattering. Neutral components of the implantation beam will tend to make the amount retained greater than the measured dose, while sputtering will have the opposite effect.

Implants of Au into copper along the ⟨110⟩ channeling direction have also been performed at 15 °K,[6] which is below the temperature for a close-pair interstitial migration in copper.[12] These studies were only performed at lower doses (2×10^{15} Au cm^{-2}), and also showed the 100% substitutionality seen in the room-temperature implanted samples. We conclude that the Au substitutionality is produced by the implantation process itself (possibly involving damage interaction) and not by any thermal diffusion or damage interaction process *following* the implantation. This will be discussed in more detail at the end of Sec. III C.

B. W in Cu

The binary system W: Cu is reported[13] to be a system with no mutual solubility and thus contrasts with the system Au: Cu which shows complete solubility.[13] We previously reported[6] that room-temperature implants of 10^{16} W cm^{-2} in Cu were ~90% substitutional and that annealing at 500 °C for 1 h reduced the substitutionality to 70%. To examine the dose dependence of implanted W in Cu, a Cu sample was mounted in a cooled goniometer capable of *in situ* W implantation and channeling analysis at 40–60 °K. No difference was found between the 60 °K results reported and identical measurements on room-temperature implanted samples. Also no change was observed upon annealing the 60 °K samples to room temperature. In Fig. 5 are shown ⟨110⟩ aligned and random spectra for the Cu sample after 60 °K ⟨110⟩ implanation of 2.0×10^{15}, 1.2×10^{16}, and 1.1×10^{17} W cm^{-2}. These values give the number of implanted ions calculated from the integrated charge. The number of implanted W actually remaining in the target after implantation is listed beside each of the spectra in Fig. 5. The 10^{15} and 10^{16} implants both exhibit the high substitutionality and extended impurity depth distributions characteristic of the previous results. The spectra for the 10^{17} cm^{-2} implant show quite different behavior. The implanted tungsten atoms are now mainly contained in a thin (~200 Å) layer. There is no decreased yield of the scattering from W atoms in this layer when the analyzing beam is aligned with the Cu ⟨110⟩ axis indicating a low ($S\sim0$) substitutionality. The copper aligned spectrum shows evidence of a surface disordered layer of Cu (peak near channel No. 350) whose thickness agrees with the thickness of the layer containing the W. In the energy region between channels 375 and 400 there is evidence of some substitutionality of W at depths beyond this surface disordered layer.

In Fig. 6 are shown ⟨110⟩ angular distributions for the implants discussed above and whose random and aligned spectra were shown in Fig. 5.

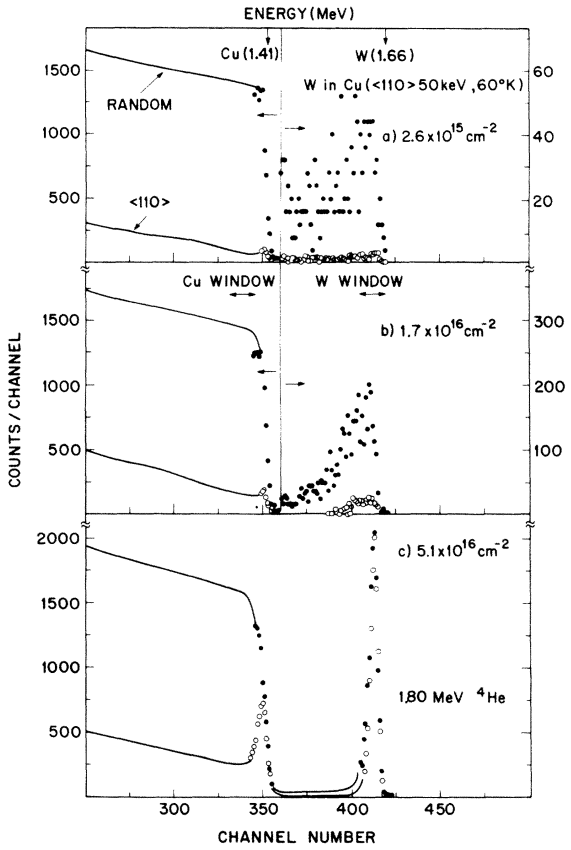

FIG. 5. Random and ⟨110⟩-aligned spectra of Cu implanted at 60 °K along the Cu ⟨110⟩ axis with W atoms. The measured amount of W retained in the Cu are (i) 2.6×10^{15} cm^{-2}, (ii) 1.7×10^{16} cm^{-2} and (iii) 5.1×10^{16} cm^{-2}. The random spectrum of Fig. 5(a) has been multiplied by 4 to normalize analysis doses.

The position and width of the energy windows used to obtain the angular distributions are indicated by double-ended arrows in Fig. 5. The 2×10^{15} cm^{-2} angular distribution is seen to indicate 100% substitutionality. Increasing the implanted dose to 10^{16} cm^{-2} causes the minimum yield of the W scattering to rise above the minimum yield of Cu, so that the calculated substitutionality is 90%. The 10% of the W atoms not on regular sites are believed to occupy random sites within the lattice. However, W precipitation is not observed.[14] The angular width of the W distribution is the same as the Cu distribution indicating that the substitutional W atoms are actually on Cu lattice sites and not slightly displaced. The angular distribution from the 10^{17} cm^{-2} W implant indicates that the W atoms in the surface layer are not located on well-defined sites within the Cu lattice. Because of the shallowness of the 10^{17} cm^{-2} W depth distribution, shown in Fig. 5(c), it is difficult to assign the Cu energy windows to derive the angular distribution, i.e., the width of the implant distribution is less than or equal to the depth resolution of the system. The copper host angular distribution is therefore weighted by the less-disordered lattice at slightly deeper depths. This may also hold true for the W angular distribution. In fact there is some evidence from the spectra in Fig. 5(c) that the copper may be totally disordered in a narrow surface layer < 100 Å thick.

The correlation between the lattice-site location and the depth distribution of W in Cu is striking. Between implant doses of 10^{16} and 10^{17} W cm^{-2}, the W becomes confined to a thin surface region which is disordered. Because the surface layer is disordered, the lack of well-defined sites for the W is understandable. There are two possible explanations for this behavior. First, the tungsten may be precipitating into agglomerates of size ≤ 200 Å and the disordered copper is due to lattice mismatch and strain. Secondly, it is possible that the high concentration of W enables the Cu to exist in a disordered state, stabilized by the presence of the W. Recent transmission electron microscopy results on these samples after 60 °K implantation of 10^{17} cm^{-2} W and annealing to room temperature indicate that there are no precipitates of dimension $\gtrsim 10$ Å and that there is no evidence of polycrystalline Cu.[14] This suggests the possibility of the formation of a thin amorphous metastable phase.

C. Lattice location of other heavy impurities in Cu

In an attempt to define the systematics of lattice site location for heavy impurities in Cu, a number of impurities were implanted at energies ranging from 50–150 keV in ⟨110⟩ channeling directions. The implanted dose in all cases was 1.0×10^{16} cm^{-2}. All implantations and analyses were performed at room temperature except as noted. The backscattering spectra taken after implanta-

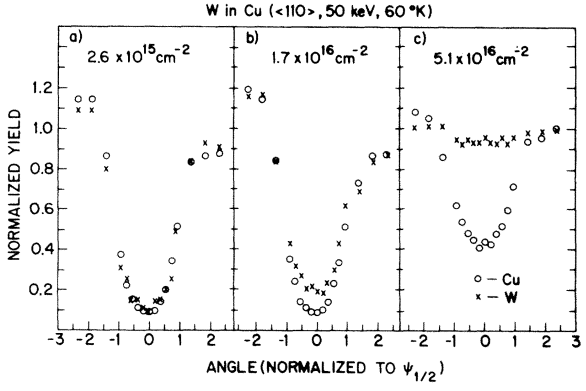

FIG. 6. ⟨110⟩ angular distributions for the spectra shown in Fig. 5.

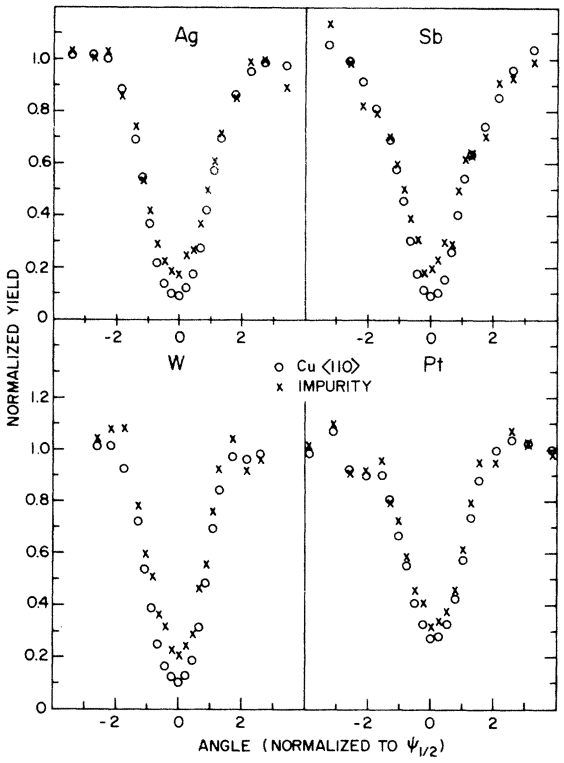

FIG. 7. ⟨110⟩ angular distributions from Cu samples implanted at room temperature with 10^{16} cm^{-2} Ag, Sb, W, and Pt.

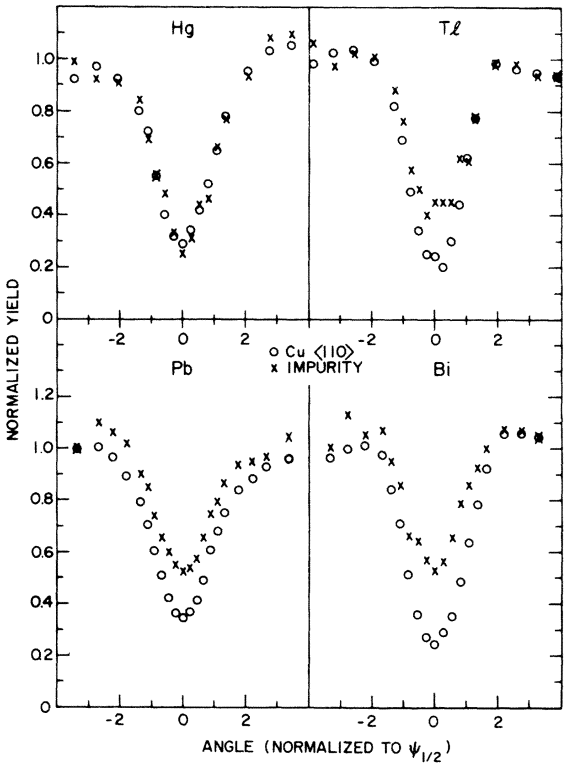

FIG. 8. ⟨110⟩ angular distributions from Cu samples implanted at room temperature with 10^{16} cm^{-2} Hg, Tl, Pb, and Bi.

tion indicated that all the implanted impurity distributions showed the extended depth behavior characteristics of channeled implants. The angular distributions for eight heavy metallic impurities are shown in Figs. 7 and 8. In all cases the distributions show significant substitutional behavior. Hg in Cu is 100% substitutional, whereas Bi in Cu is only about 60% substitutional. All of the impurities for which data are shown in Figs. 7 or 8, except Bi, show the same width of the ⟨110⟩ dip as the Cu host. The width of the Bi dip is significantly narrower than the Cu dip, leading to the conclusion that Bi atoms are slightly displaced from normal Cu lattice sites.[15]

Lattice-location measurements of I and Xe in Cu gave quite different results from the heavy metallic impurity implants described above. The results of I are seen in Fig. 9. The behavior of I is a function of the depth and thus the local concentration of I atoms. Near the surface there is no substitutionality of I. The aligned scattering spectrum exhibits no evidence of a disordered surface layer in the copper scattering as was seen in the case of the 10^{17} cm^{-2} W data, however. The peak I concentration in this surface region is ~1.5 at.%. At 1000 Å depth, where the localized I concentration has decreased to 0.5 at.%, the angular scan shows that the I is up to 70% substitutional, but that the dip is very significantly narrowed indicating a small displacement of the I atoms from Cu lattice sites.

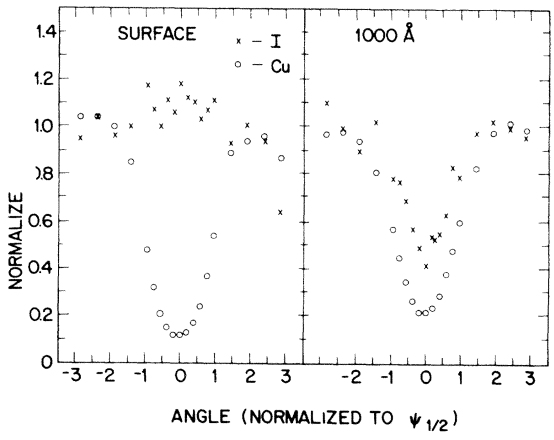

FIG. 9. ⟨110⟩ angular distributions from a Cu sample implanted at room temperature with 10^{16} I cm^{-2}. The distribution on the left is taken near the surface (0–400 Å), the distribution on the right is taken at a depth of ~1000 Å.

TABLE I. Summary of substitutionality results and physical properties for impurities implanted in copper.

Element	Ag	Sb	I	Xe	W	Pt	Au	Hg	Tl	Pb	Bi
Substitutionality	0.93	0.93	0.0–0.70	0.0	0.90	0.92	1.00	1.00	0.84	0.72	0.62
Damage (host χ_{min})	0.09	0.09	0.10	0.10	0.20	0.25	0.09	0.20	0.22	0.30	0.25
$\psi_{1/2}(\text{imp})/\psi_{1/2}(\text{Cu})$	1.0	1.0	0.7	0.0	1.0	1.0	1.0	1.0	1.0	1.0	0.83
Goldschmidt radius ($R_{Cu}=2.55$)	2.9	2.9–3.4	•••	•••	2.8	2.8	2.9	3.0	3.4	3.5	3.2–3.5
Electronegativity ($EN_{Cu}=1.9$)	1.9	1.9	2.5	•••	1.7	2.2	2.4	1.9	1.8	1.8	1.8

Implanted Xe showed a completely random behavior regardless of the dose, depth of analysis, or temperature of implantation. Similar results were obtained for channeling measurements along the ⟨100⟩ and ⟨111⟩ axes. Implantations at temperatures as low as 9 °K to a dose of 1×10^{15} Xe cm^{-2} showed the same behavior as room-temperature implanted samples.

The results of all the lattice location measurements in Cu are summarized in Table I. Along with the experimentally determined parameters of substitutionality, Cu lattice damage and relative widths of the impurity and lattice angular distributions are listed the Goldschmidt radius and the electronegativity for those impurities where they are defined. The experimental error on the substitutionalities is ± 1%–2%. For electronegativity, no correlation with the substitutionality exists. There is no clear correlation between the Goldschmidt radius and substitutionality, but the very large atoms (Tl, Pb, and Bi) show the lowest substitutionality for the impurities listed and for which the Goldschmidt radius is defined.

The equilibrium phase diagrams[13,16,17] of the various metallic impurities and copper range from complete solubility in the case of Au and Pt to complete immiscibility in the case of W. Under equilibrium conditions a high mutual solubility would imply a high substitutionality and a very low solubility would lead to low substitutionality, but indeed all metallic impurities appear to have a relatively high probability of occupying substitutional sites regardless of the solubility. The only impurities investigated which showed evidence of low substitutionality were the nonmetallic impurities I and Xe.

The observation that all metallic impurities tend to occupy highly substitutional sites upon implantation into Cu, regardless of their chemical type, suggests that dynamical processes near the end of range of the implanted atoms may govern the lattice site location. We suggest that an isolated Cu vacancy is a local potential minimum for implanted metal atoms, and perhaps for I also if the local I concentration is low enough. As such an impurity atom slows to rest during the implantation process, it can end up on a lattice site via a replacement collision or by diffusional motion due to the localized lattice energy transient due to the collision cascade (thermal spike). Recent calculations[18] of the probability of replacement collisions show high probabilities (50%–80%) for incident ions in the mass range studied here suffering replacement collisions at the end of range (see Appendix). By this model, however, Xe should show some substitutionality for low dose, low-temperature implantation and we find Xe to be entirely nonsubstitutional. Thus we conclude that a copper lattice vacancy is not a local potential minimum for Xe atoms. The fact that implanted Au is 100% substitutional in Cu when implanted and analyzed below 15 °K (although the replacement collision probability is only ~55%) indicates that processes other than replacement collisions must be operative, probably processes dependent upon the high "local lattice temperature" near the core of the collision cascade. Thompson[19] has suggested that during the lifetime of such a thermal spike (typically 10^{-11} to 10^{-12} sec), interstitial-vacancy recombination can be expected due to a localized rise in the lattice temperature, whereas vacancy migration is not predicted due to the high activation energy. The true situation is probably a combination of replacement collisions and recombination of the implanted impurity with copper vacancies which is enhanced by the high localized thermal energy.

Metastability of substitutional solid solutions is well known. Rapid quenching of a liquid-metal alloy can cause the liquidus-solidus to be crossed so quickly that second-phase nucleation and growth is suppressed. This has been experimentally seen as the extension of terminal solid solubility limits following rapid quenching from the liquid state.[20] Lattice parameter versus concentration curves[20] gave deviations from Vegard's law which could

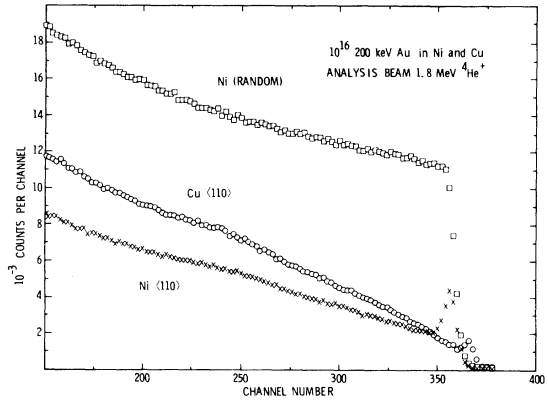

FIG. 10. Random and ⟨110⟩-aligned spectra for a Ni sample implanted with 10^{16} Au cm^{-2}. Also shown is the ⟨110⟩-aligned spectrum from a Cu sample after an identical implant.

be predicted by extrapolating the equilibrium data. This indicated the single phase present was a complete solid solution lending support to our suggestion that a lattice vacancy is a local potential minimum for metallic impurity atoms, even for systems which are immiscible under equilibrium conditions.

D. Dechanneling

In Fig. 10 are shown a ⟨110⟩-aligned spectrum for Cu implanted with 10^{16} 200 keV Au cm^{-2} as

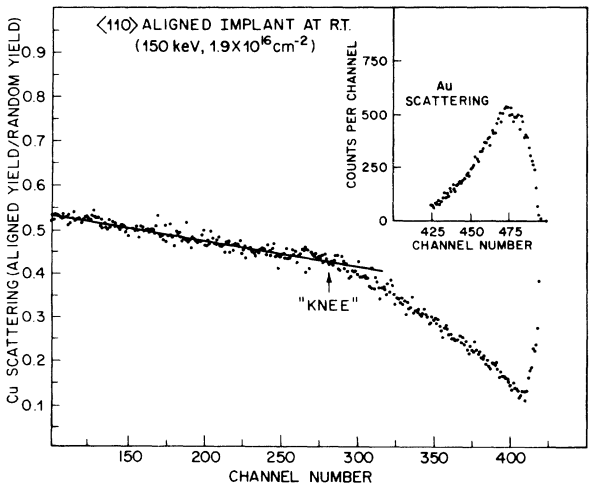

FIG. 11. Aligned yield/random yield for Cu implanted with 10^{16} Au cm^{-2} at room temperature along a ⟨110⟩ channel. The inset shows the scattering yield from Au atoms normalized such that the Au surface scattering is at the same energy (channel number) as the Cu surface scattering.

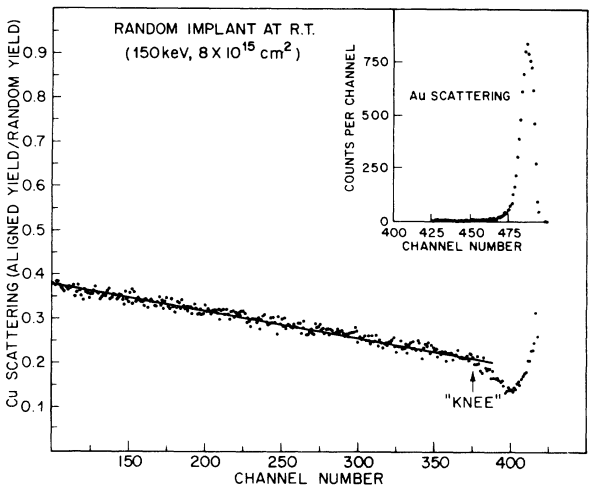

FIG. 12. Aligned yield/random yield for Cu implanted with 10^{16} Au cm^{-2} at room temperature in a random direction. The inset shows the Au scattering normalized as in Fig. 11. The data shown in here are taken from the spectra shown in Fig. 2.

well as random and ⟨110⟩-aligned spectra for Ni after an identical implant. The minimum yield for Cu (10%) is significantly lower than that for Ni (20%) and the Ni-aligned spectrum shows evidence of a thin layer of disordered Ni at the surface. Both aligned spectra show a "knee" near channel No. 240, but the aligned yield in the Cu sample increases much faster as a function of depth than that for the Ni and is actually above the Ni aligned yield except very near the surface. Similar knees have been observed in ion-implanted metal crystals by Gettings *et al.*[21,22] and by Sood and Dearnaley.[23] Generally these knees have been recognized to be the end of a layer of dechanneling centers introduced during high-dose implantations into metals.

The knees are accentuated if one plots the aligned yield divided by the random yield as a function of depth (channel number). Figure 11 is such a plot for a channeled implant of Au in Cu and Fig. 12 is a plot of an identical random implant of Au in Cu. Figure 12 uses the same data used in Fig. 2. The reason less Au is retained in the randomly implanted sample than in the channeled implanted sample is increased sputtering combined with the much shallower implanted distribution for the random case. In both cases, the knee occurs at a depth corresponding to the approximate end of range of the implanted impurity as seen by the Au scattering shown in the inset. The surface channels for Au scattering and Cu scattering have been normalized and kinematical effects contributing to different energy-to-depth conversions for scattering from Cu and from Au are small.

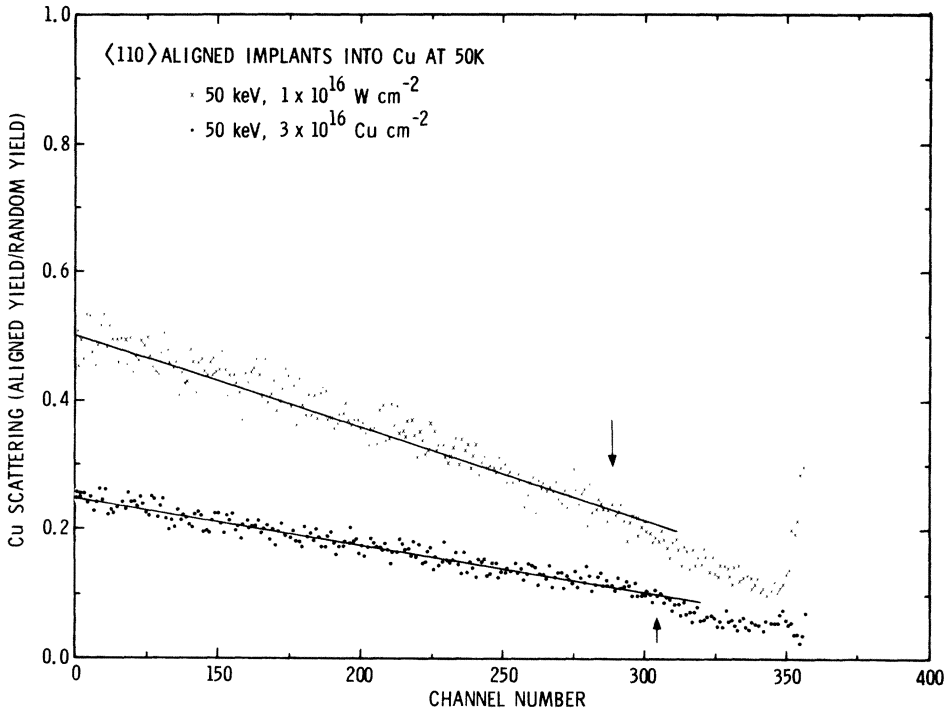

FIG. 13. Aligned yield/random yield for Cu implanted with 3×10^{16} Cu cm^{-2} at room temperature along a ⟨110⟩ channel (·). Also shown are data for 1×10^{16} W cm^{-2} implanted under identical conditions (×).

A comparison of dechanneling depths and implanted-impurity depth distributions leads to the conclusion that the layer of dechanneling centers is coincident with the implanted layer. This could be due to Cu damage created by the implantation but not specifically associated with the implanted atoms or to localized strains in the Cu lattice around the implanted species after they come to rest. In Fig. 13 are shown the aligned yield divided by the random yield for a 1×10^{16} cm^{-2} implantation of 50-keV W into Cu. The gain settings were different for these spectra from those of Figs. 11 and 12 leading to a different channel for Cu scattering at the surface. Whereas the dechanneling in the W-implanted sample is comparable with that which we observed for the Au implantations, the Cu implanted sample has a much lower level of dechanneling.

Brice[24] has developed a technique for calculating the depth distribution of energy deposited into atomic processes. The calculation is for an amorphous target and thus the depth distributions are not meaningful for the channeled implants in this work. The Brice calculations yield 0.64 and 0.67 as the fractions of the incident energy which ultimately are converted into atomic damage for 50-keV Cu and W, respectively, incident on a copper target. Thus equal doses of Cu and W should produce about the same amount of lattice damage in an amorphous copper target. We will assume that the amount of damage would also be comparable for channeled W and Cu implantations. As indicated in Fig. 13, however, the dechanneling from a 3×10^{16} cm^{-2} Cu implantation at 40 °K is appreciably less than the dechanneling from a 1×10^{16} cm^{-2} W implantation at 40 °K. These doses were measured by current integration since the actual amount of implanted Cu cannot be measured by backscattering. The Cu implantation deposited about three times the energy into atomic processes as compared with the W implantation. Since the dechanneling from the copper crystal was less after the Cu implantation than after the W implantation we conclude that the dechanneling is associated primarily with the implanted impurities and not with copper lattice damage caused by the implantation.

It has been suggested[20-22] that the knees in the channeling spectra are indicative of the long-range migration of a Cu defect during implantation, but the results here lend support to the simple interpretation that the knees are due to dechanneling associated with the implanted impurity itself.

IV. CONCLUSIONS

This study has demonstrated some unique features of the alloy systems created by ion implantation into metals, specifically copper. It has been demonstrated that 100% substitutional alloys can be formed by implantation and that for doses $\sim10^{16}$ atoms cm^{-2}, implanted metal ions tend to occupy Cu lattice sites with a high probability. Highly substitutional nonequilibrium alloy layers can be formed even for systems where equilibrium formation is not predicted. It is thus demonstrated

TABLE II. Replacement collision probabilities for ions of various atomic numbers in copper.

Copper target (E_d = 25 eV)	
Z_1 (atomic number of projectile)	P (probability of a replacement collision)
10	0.20
20	0.62
30	0.79
40	0.81
50	0.79
60	0.73
70	0.65
80	0.55

that classical parameters such as atomic size and electronegativity cannot be used to predict the substitutionality of ion-implanted metallic impurities. We have suggested that this phenomenon is a combination of replacement collisions events and localized motion of the implanted ion caused by the collision cascade. Thermal motion of the ions for times greater than about 10^{-10} sec (the lifetime of the thermal spike) after the implantation event has been ruled out by low-temperature implantation experiments. In fact there is no apparent implantation temperature dependence of the substitutionality of Au, Xe, and W implanted in Cu between 15 °K and room temperature. We have studied two systems, Au in Cu and W in Cu, at high implantation concentrations >10 at.%. Au still remains substitutional in Cu, but W no longer occupies regular Cu lattice sites. We have as yet no detailed understanding of why W implanted into Cu can be 100% substitutional at low concentrations with little lattice damage but produce a disordered layer of W in Cu, with no regular W lattice sites, for the higher concentrations.

For the two nonmetal implantations, Xe and I, the lattice sites are very different from those observed for the metallic implantations. Xe, an insert gas, demonstrates no substitutionality; similarly I, a halogen, although occupying regular copper lattice sites at low doses, does not occupy those sites for localized concentrations $\gtrsim 1$ at.%. The disparity between the I and Xe results and those for metals is not surprising in light of the completely different bonding mechansims or lack thereof.

The levels of damage observed in these samples are very low considering the high-dose implants, and most of the damage appears to be in the form of a layer of dechanneling centers which is coincident in depth with the layer containing the implanted atoms. Since the dechanneling observed for Cu implants into Cu is much lower than that observed for implants of heavy impurities into copper, it is suggested that the dechanneling centers are Cu atoms slightly off normal copper lattice sites due to the high localized strain near an implanted impurity.

These studies have shown that metastable phases are achievable by room-temperature implantation. Future work will require correlation of lattice site location results with measurements which can probe the crystal microstructure in the implanted layer. Electron microscopy work is now in progress to obtain such results.

ACKNOWLEDGMENTS

We would like to thank J. H. Smalley, C. T. Fuller, and J. M. McDonald for their assistance with the implantations and analyses. The collaboration of W. J. deBonte and W. M. Augustyniak in the initial stages of this work is acknowledged. The use of the unpublished data of D. K. Brice and A. G. Cullis is appreciated. We are indebted to S. M. Myers for valuable discussions on the microstructure of metals under irradiation.

APPENDIX: REPLACEMENT COLLISIONS

As an energetic atom comes to rest in a solid it loses energy to the solid via atomic and electronic scattering. In some collisions with the target atoms the moving atom may displace a host atom from its lattice site, but not retain enough energy to escape from that site after the collision. Such an event is called a replacement collision. Owing to the requirement of conservation of energy and momentum these collisions are most likely to occur at energies near the displacement threshold energy E_d.

Brice has generalized a technique due to Dederichs *et al.*[25] and derived an integral equation which governs the probability that a replacement collision will occur as an incident particle of energy E comes to rest in the solid. In numerical solutions to this equation, he has used Lindhard's elastic-scattering cross section (which is based on a Thomas-Fermi model of the atom) and a maximum impact parameter of $\frac{1}{2}$ the nearest-neighbor distance. For low incident energies the probability of an atom experiencing a replacement collision rises sharply from zero at $E = E_d/\gamma$ and then oscillates with further increases in the energy, eventually becoming a constant at $E \sim 100\, E_d$. [Here γ is the maximum fractional energy transfer $4m_1m_2/(m_1+m_2)^2$ in an elastic collision of incident and target atoms.] For a copper target, the high-energy replacement collision probabilities are tabulated in Table II.

*The work performed at Sandia Laboratories was supported by the United States Energy Research and Development Administration, ERDA.

[1]*Applications of Ion Beams to Metals*, edited by S. T. Picraux, E. P. EerNisse, and F. L. Vook (Plenum, New York, 1974).
[2]*Channeling*, edited by D. V. Morgan (Wiley, London, 1974).
[3]D. S. Gemmell, Rev. Mod. Phys. 46, 129 (1974).
[4]A recent compilation of lattice-location results by channeling can be found in S. T. Picraux in *New Uses of Low-Energy Accelerators*, (Plenum, New York, 1975).
[5]J. A. Borders, J. M. Poate, and W. J. deBonte, Bull. Am. Phys. Soc. 19, 257 (1973).
[6]J. M. Poate, W. J. deBonte, W. M. Augustyniak, and J. A. Borders, Appl. Phys. Lett. 25, 698 (1974).
[7]J. A. Cairns *et al.*, Radiat. Eff. 12, 7 (1972).
[8]A. Van Wijngaarden *et al.*, Can. J. Phys. 47, 411 (1969).
[9]J. Lindhard, Mat. Fys. Medd. Dan. Vid. Selsk. 34 No. 14 (1965).
[10]R. B. Alexander, P. A. Callagan, and J. M. Poate, Phys. Rev. B 9, 3022 (1974).
[11]D. K. Brice, (unpublished data).
[12]W. Schilling *et al.*, in *Vacanies and Interstitials in Metals*, edited by A. Seeger *et al.* (North Holland, Amsterdam, 1970).
[13]M. Hanson, *Constitution of Binary Alloys*, 2nd ed. (McGraw-Hill, New York, 1958).
[14]A. G. Cullis, J. M. Poate, and J. A. Borders (unpublished).
[15]S. T. Picraux, W. L. Brown, and W. M. Gibson, Phys. Rev. B 6, 1382 (1972).
[16]R. P. Elliot, *Constitution of Binary Alloys, First Supplement* (McGraw-Hill, New York, 1965).
[17]F. A. Shunk, *Constitution of Binary Alloys, Second Supplement* (McGraw-Hill, New York, 1969).
[18]D. K. Brice, (unpublished data).
[19]M. W. Thompson, *Defects and Radiation Damage in Metals*, (Cambridge U. P., London, 1969).
[20]P. Duwez, in *Progress in Solid State Chemistry*, edited by H. Reiss (Pergamon, Oxford, 1967), Vol. 3.
[21]M. Gettings, O. Meyer, and G. Linker, Radiat. Eff. 21, 51 (1974).
[22]M. Gettings, K. Langguth, and G. Linker, in *Applications of Ion Beams to Metals*, edited by S. T. Picraux *et al.* (Plenum, New York, 1974), p. 241.
[23]D. Sood and G. Dearnaley, J. Vac. Sci. Technol. 12, 445 (1975).
[24]D. K. Brice, Radiat. Eff. 6, 77 (1970); J. Appl. Phys. (to be published).
[25]P. H. Dederichs *et al.*, Phys. Status Solidi 8, 213 (1965).